Journal of Organometallic Chemistry, 473 (1994) 265–272

Reaction of $RuH_2(PMe_3)_4$ with benzaldehyde. Formation of novel oxametallacycle and metallacycloketone complexes via C–H bond activation of aldehyde

Fumiyuki Ozawa [a], Isao Yamagami [b] and Akio Yamamoto [c]

[a] *Catalysis Research Center, Hokkaido University, Kita-ku, Sapporo 060 (Japan)*
[b] *Research Laboratory of Resources Utilization, Tokyo Institute of Technology, 4259 Nagatsuta, Midori-ku, Yokohama 227 (Japan)*
[c] *Department of Applied Chemistry, School of Science and Engineering, Waseda University, Shinjiku-ku, Tokyo 169 (Japan)*

(Received December 8, 1993; in revised form February 16, 1994)

Abstract

The PMe_3-coordinated ruthenium dihydride complex $RuH_2(PMe_3)_4$ (**1**) reacted with PhCHO in toluene at −20°C to give an oxaruthenacycle complex (**2**) and 1 equivalent of $PhCH_2OH$. The same reaction carried out at elevated temperatures, on the other hand, afforded a ruthenacycloketone complex (**3**). Complexes **2** and **3** were characterized by means of IR and NMR spectroscopy and elemental analysis. An X-ray diffraction study revealed that complex **2** has an oxametallacycle structure associated with benzyl alcohol by a hydrogen bond. Crystal data for **2**: orthorhombic, space group $Pnb2_1$, $a = 13.580(1)$ Å, $b = 18.220(2)$ Å, $c = 12.540(1)$ Å, $V = 3102.7(5)$ Å^3, $Z = 4$.

Key words: Ruthenium; Hydride; Metallacycle; Aldehyde; Hydrogen bonding; Dimerization

1. Introduction

Triphenylphosphine-coordinated ruthenium dihydride, $RuH_2(PPh_3)_4$, serves as an efficient catalyst for the Tishchenko-type dimerization of aldehydes to give esters (eqn. (1)) [1,2]. This reaction was assumed to proceed by a catalytic process as illustrated in Scheme 1 [1]. Ruthenium dihydride **A**, employed for the catalytic reaction, undergoes insertion of aldehyde into the Ru–H bond. Reductive elimination of alcohol from the resulting alkoxo(hydrido)ruthenium complex (**B**) generates a Ru^0 species **C**, which is active in the catalytic reaction. Oxidative addition of aldehyde to **C** forms an acylruthenium hydride (**D**). Insertion of another molecule of aldehyde into the Ru–H bond in **D** gives an acyl(alkoxo)ruthenium(II) complex (**E**), which reductively eliminates ester, regenerating Ru^0 species **C** that carries the catalytic cycle.

$$2RCHO \xrightarrow{RuH_2(PPh_3)_4} RCO_2CH_2R \qquad (1)$$

The catalytic process depicted in Scheme 1 seems reasonable in view of the precedents of oxidative addition of the formyl group in aldehyde to low-valent transition metal complexes [3], of insertion of the carbonyl group in aldehyde and ketone into a late transition metal–hydride bond [4], and of reductive elimination of acyl–alkoxide complexes to give esters [5]. However, since the catalytic reaction using the PPh_3-coordinated ruthenium catalyst proceeds very rapidly, it was not feasible to obtain direct evidence for the catalytic intermediates **B–E**. In this study, we examined the catalytic dimerization of benzaldehyde using PMe_3-coordinated ruthenium catalyst $RuH_2(PMe_3)_4$ (**1**) [6]. The use of basic PMe_3 as the stabilizing ligands provided a convenient reaction rate for examining the catalytic system by NMR spectroscopy and allowed us to gain an insight into the catalytic mechanism.

2. Results

2.1. Reactions of $RuH_2(PMe_3)_2$ (1) with benzaldehyde

The PMe_3-coordinated ruthenium dihydride **1** was treated with an excess amount of benzaldehyde in

Correspondence to: Professor A. Yamamoto.

0022-328X/94/$7.00
SSDI 0022-328X(94)24597-C

toluene-d_8 or benzene-d_6 and the reaction was followed by ^1H and $^{31}P\{^1H\}$ NMR spectroscopy. The reaction products varied markedly with the reaction temperature employed (eqn. (2)).

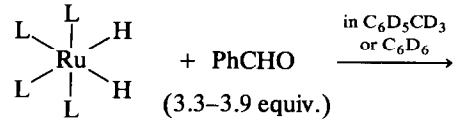

(1: L = PMe_3)

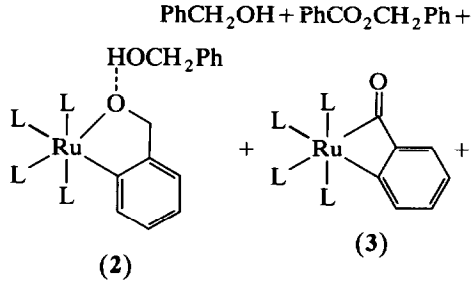

(2)

Table 1 summarizes the typical results. At −20°C, the reaction proceeded very slowly (entry 1). The $^{31}P\{^1H\}$ NMR spectrum of the reaction solution after 16 days exhibited A_2MX signals assignable to the oxaruthenacycle complex **2** (59%) and signals of some unidentified Ru–PMe_3 species (total 41%). ^1H NMR analysis of the same solution showed partial conversion of benzaldehyde (185% with respect to **1** used) and the formation of benzyl alcohol (103% yield based on **1** used), whereas no benzyl benzoate was observed. As is shown in the following section, benzyl alcohol generated in the reaction system is associated with **2** by a hydrogen bond.

When the reaction was carried out at room temperature, the ruthenacycloketone complex **3** was formed in addition to **2** (entry 2). At this temperature, the formation of benzyl benzoate and benzyl alcohol was observed. At 100°C complex **3** was obtained in 26% yield, whereas no trace of **2** was detected in the reaction system (entry 3). In this case 74% of **1** remained unreacted in the reaction solution and catalytic formation of benzyl benzoate (427% yield based on **1** consumed) proceeded.

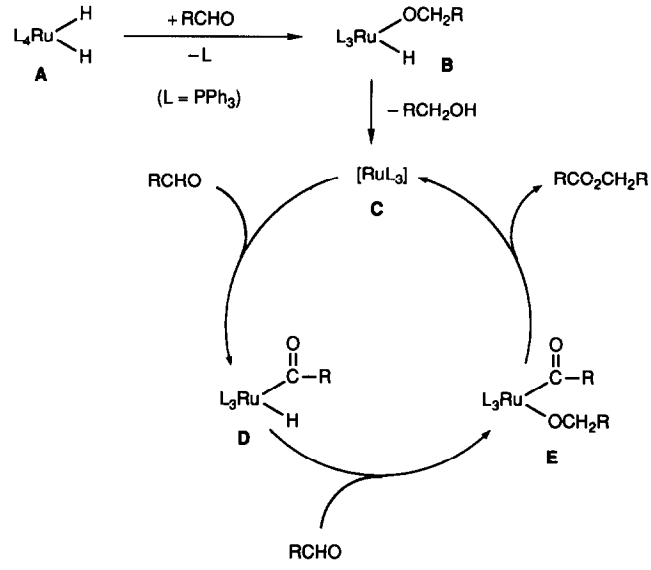

Scheme 1.

2.2. Isolation and characterization of complexes 2 and 3

Complex **2** was isolated as a white solid by slow cooling of the reaction solution of entry 1 in Table 1 (40%). Recrystallization of the crude product from cold toluene gave colourless crystals of **2** suitable for X-ray diffraction study.

Isolation of complex **3** was performed by the follow-

TABLE 1. Reactions of $RuH_2(PMe_3)_4$ (**1**) with PhCHO [a]

Entry	Starting materials (mmol)		Reaction temperature (°C)	Products						
				Organics (mmol) [b]			Complexes (%/1) [c]			
	1	PhCHO		$PhCH_2OH$	$PhCO_2CH_2Ph$	PhCHO [d]	2	3	Others	1 [e]
1	0.34	1.33	−20	0.35 [f]	0.00	0.70	59	0	41	0
2	0.11	0.36	Room temp.	0.06 [f]	0.10	0.02	41	29	0	30
3	0.18	0.63	100	0.12	0.20	0.10	0	26	0	74

[a] The reaction was performed in toluene-d_8 (entry 1) or benzene-d_6 (entries 2 and 3). Reaction time: 16 days (entry 1), 6 days (entry 2) and 5 h (entry 3).
[b] Determined by ^1H NMR spectroscopy.
[c] Determined by $^{31}P\{^1H\}$ NMR spectroscopy.
[d] The amount of benzaldehyde unreacted.
[e] The amount of complex **1** unreacted.
[f] Part of the benzyl alcohol combines with **2** by a hydrogen bond. See text.

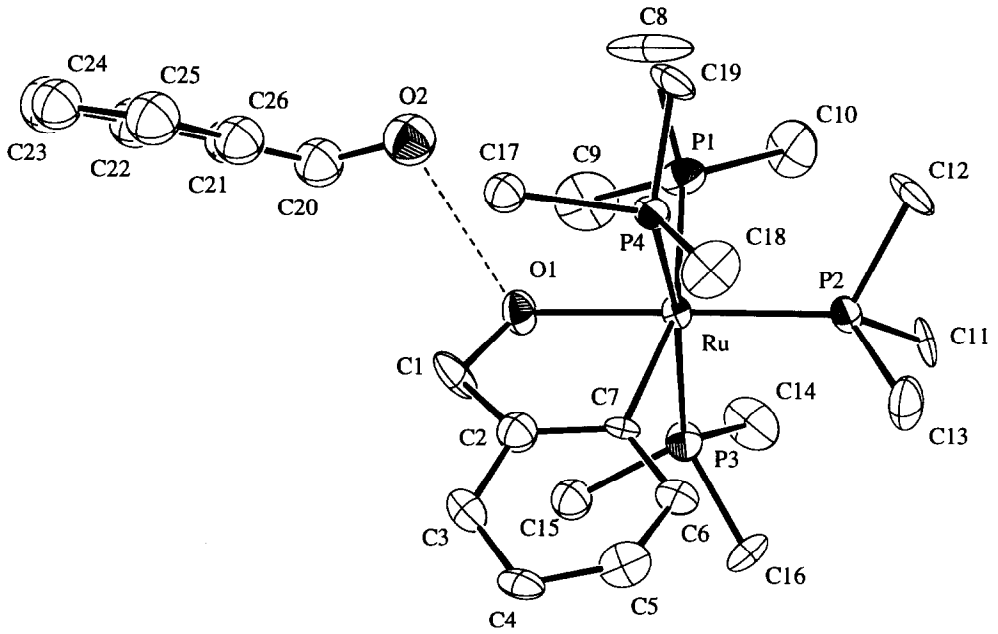

Fig. 1. An ORTEP view of complex **2**. The thermal ellipsoids are drawn at the 30% probability level.

ing procedure. A toluene solution containing **1** and 10 equivalents of PhCHO was stirred at room temperature for 4 days. At this stage the reaction mixture contained complexes **2** and **3**. The mixture was then heated at 100°C for 5 h to convert **2** into **3**. Cooling the resulting reaction solution to −20°C gave rise to the formation of pale yellow needles of **3** (33%), which contained 1 equivalent of benzyl alcohol in the crystal.

Complexes **2** and **3** were characterized by means of elemental analysis and IR and NMR spectroscopy. Characterization of **2** was performed also by X-ray diffraction study. Figure 1 shows the X-ray structure of **2**. The bond distances and angles are listed in Table 2. As can be seen from Fig. 1, complex **2** has an oxametallacycle ring associated with benzyl alcohol by a hydrogen bond. The distance between O1 and O2 atoms is 2.75(2) Å, the value being typical of an O–H···O hydrogen bond [7–9]. The five-membered oxaruthenacycle ring including Ru, O1, C1, C2 and C7 is almost flat, the sum of the interior angles being 538.5°. The complex has a distorted octahedral structure with two equatorial PMe_3 ligands (P1 and P2) and two axial PMe_3 ligands (P3 and P4).

Table 3 lists the characteristic NMR and IR data for **2** and **3** [10*]. The presence of a hydrogen bond in **2** in the solid state was also indicated by appearance of sharp peaks at 2740 and 2664 cm^{-1} in the IR spectrum. In the ^1H NMR spectrum of **2**, the OH proton was observed as a broad signal at considerably lower magnetic field (δ 7.47) than that of free benzyl alcohol (δ 4.34), showing the hydrogen bonding taking place in solution also. In the $^{13}C\{^1H\}$ NMR spectrum, the phenyl carbon bonded to ruthenium (C^{10}; see the numbering in Table 3) appeared at δ 179.4 as a doublet of doublets owing to the coupling to the non-equivalent phosphorus nuclei of the equatorial PMe_3 ligands. All other NMR data for **2** were fully consistent with the X-ray structure.

Since a single crystal of **3** suitable for X-ray diffraction study could not be obtained, the structure was assigned based on the NMR and IR data listed in Table 3. Although this complex was isolated as a 1:1 mixture with benzyl alcohol, the spectroscopic data indicated that no association of **3** with benzyl alcohol by a hydrogen bond exists in the solid or in solution. Thus, in the ^1H and ^{13}C NMR spectra measured in CD_2Cl_2 solution, benzyl alcohol released from the crystals of **3** showed almost the same chemical shifts and coupling patterns as the free alcohol that were independently observed. In the IR spectrum (KBr disc), a broad peak assignable to the ν_{OH} band was observed around 3200–3600 cm^{-1}, the value being in the typical range for free alcohols.

The A_2MX signals that appeared in the $^{31}P\{^1H\}$ NMR spectrum clearly showed that complex **3** has an octahedral structure similar to that of **2**. The ^1H and ^{13}C NMR data for the PMe_3 ligands (one virtual triplet

* Reference numbers with asterisks indicate a note in the list of references.

and two doublets) also supported this structural assignment. The presence of a ruthenacycloketone ring was strongly suggested by the appearance of a doublet at δ 182.0 and a doublet of doublets at δ 179.4 in the $^{13}C\{^1H\}$ NMR spectrum, which are assigned to the carbonyl and phenyl *ipso* carbons, respectively, bonded directly to ruthenium (C^4 and C^{10}). In the ^1H NMR spectrum, the four protons (H^6, H^7, H^8 and H^9) of the phenyl ring were observed non-equivalently at δ 6.88, 7.02, 7.47 and 7.61, respectively. Among them the signal of the lowest chemical shift (H^9) showed apparent coupling toward the phosphorus nuclei, though the detailed coupling pattern was obscure owing to broadening of the peak.

TABLE 2. Bond distances (Å) and angles (°) for the oxaruthenacycle complex **2**

Bond distances			
Ru–P1	2.380(4)	P2–C11	1.78(3)
Ru–P2	2.279(3)	P2–C12	1.92(3)
Ru–P3	2.320(9)	P2–C13	1.85(1)
Ru–P4	2.404(9)	P3–C14	1.99(4)
Ru–C7	2.118(11)	P3–C15	1.73(3)
Ru–O1	2.144(8)	P3–C16	1.77(3)
O1–C1	1.43(2)	P4–C17	2.01(2)
C1–C2	1.51(2)	P4–C18	1.90(3)
C2–C7	1.41(2)	P4–C19	1.78(3)
C2–C3	1.43(2)	O2–C20	1.40(3)
C3–C4	1.41(2)	C20–C21	1.53(3)
C4–C5	1.42(2)	C21–C22	1.37(3)
C5–C6	1.44(2)	C22–C23	1.45(4)
C6–C7	1.42(2)	C23–C24	1.32(4)
O1–O2	2.75(2)	C24–C25	1.42(4)
P1–C8	1.83(3)	C25–C26	1.40(4)
P1–C9	1.89(2)	C26–C21	1.43(4)
P1–C10	1.86(2)		
Bond angles			
C7–Ru–O1	78.4(4)	C15–P3–Ru	116.6(10)
C7–Ru–P1	162.0(3)	C15–P3–C16	95.2(14)
C7–Ru–P2	103.6(3)	C16–P3–Ru	117.2(9)
C7–Ru–P3	82.9(9)	C17–P4–Ru	110.8(7)
C7–Ru–P4	82.1(9)	C17–P4–C18	107.8(12)
O1–Ru–P1	83.6(3)	C17–P4–C19	90.4(13)
O1–Ru–P2	176.3(6)	C18–P4–Ru	113.8(9)
O1–Ru–P3	84.0(7)	C18–P4–C19	103.8(15)
O1–Ru–P4	92.7(7)	C19–P4–Ru	126.9(11)
P1–Ru–P2	94.5(1)	C1–O1–Ru	117.8(7)
P1–Ru–P3	97.2(4)	O1–C1–C2	109.4(10)
P1–Ru–P4	96.9(4)	C1–C2–C7	120.0(11)
P2–Ru–P3	93.1(4)	C3–C2–C7	120.7(12)
P2–Ru–P4	90.8(4)	C1–C2–C3	116.4(11)
P3–Ru–P4	165.0(3)	C2–C3–C4	120.9(12)
C8–P1–Ru	122.8(9)	C3–C4–C5	117.1(13)
C8–P1–C9	100.7(12)	C4–C5–C6	118.7(14)
C8–P1–C10	98.0(10)	C5–C6–C7	120.3(13)
C9–P1–Ru	107.9(7)	C2–C7–C6	117.7(10)
C9–P1–C10	98.4(11)	C2–C7–Ru	112.9(8)
C10–P1–Ru	124.4(7)	C6–C7–Ru	129.3(9)
C11–P2–Ru	117.2(11)	O2–C20–C21	111.8(18)
C11–P2–C12	99.1(12)	C22–C21–C26	120.6(21)
C11–P2–C13	97.4(16)	C20–C21–C22	119.1(19)
C12–P2–Ru	118.9(11)	C20–C21–C26	120.3(19)
C12–P2–C13	97.7(16)	C21–C22–C23	118.4(23)
C13–P2–Ru	121.8(5)	C22–C23–C24	122.0(26)
C14–P3–Ru	121.6(11)	C23–C24–C25	120.3(25)
C14–P3–C15	104.2(15)	C24–C25–C26	120.2(25)
C14–P3–C16	97.4(15)	C21–C26–C25	118.4(23)

2.3. *Reactions of complexes 2 and 3*

Treatment of **2** with 6 equivalents of benzyl alcohol in benzene-d_6 at room temperature for 1 day gave the dihydridoruthenium complex **1** in 65% yield (eqn. (3)). Also found in the reaction solution by $^{31}P\{^1H\}$ NMR spectroscopy were complex **3** (6%), unidentified Ru–PMe_3 species (5%) and unreacted complex **2** (24%). ^1H NMR analysis of the solution revealed formation of benzyl benzoate (71% yield based on **2** employed) and benzaldehyde (trace).

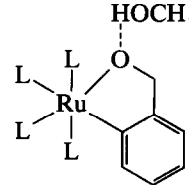

2 (0.028 mmol)

$$\xrightarrow[\text{in } C_6D_6 \text{ at room temp. for 24 h}]{+PhCH_2OH\ (0.17\ mmol)} \underset{(65\%)}{\mathbf{1}} + \underset{(24\%)}{\mathbf{2}} + \underset{(6\%)}{\mathbf{3}} + \text{other Ru species} + \underset{(71\%)}{PhCO_2CH_2Ph} + \underset{(\text{trace})}{PhCHO} \quad (3)$$

(5%)

On the other hand, complex **3** was fairly stable at room temperature in solution in the presence or absence of benzaldehyde and benzyl alcohol. Thus, no ester formation was observed with **3** at room temperature, while the complex decomposed gradually at 100°C to give unidentified ruthenium species.

3. Discussion

We isolated the novel oxaruthenacycle complex **2** and the ruthenacycloketone complex **3** from the catalytic reaction system of the Tishchenko-type dimerization of benzaldehyde into benzyl benzoate. As shown in Scheme 2, the structures of **2** and **3** are well related to those of the intermediates proposed in Scheme 1.

The formation of **2** having a benzyloxoruthenium structure at low temperature indicates the occurrence of insertion of benzaldehyde into the Ru–H bond(s) in **1**, giving benzyloxoruthenium species **F** and **G**. Orthometallation of one of the phenyl groups in **G** and the subsequent reductive elimination of benzyl alcohol forms **2**. This complex is stable in solution at −20°C, whereas at room temperature complex **2** reacted with

benzyl alcohol to regenerate dihydride complex **1** (eqn. (3)). Under such conditions where complexes **1** and **2** are reversibly interconverted, the formation of benzyl benzoate was observed. Therefore, it is likely that a Ru(0) species (**H**) that is active in the catalytic ester formation is generated from one of the intervening intermediates in the interconversion between **1** and **2**, probably from the benzyloxo–hydrido species **F**.

TABLE 3. NMR and IR data for complexes **2** and **3** [a]

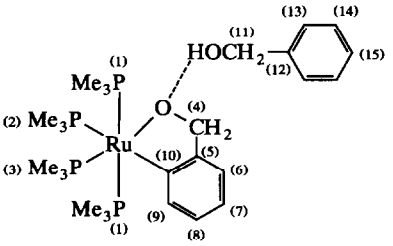

(2)

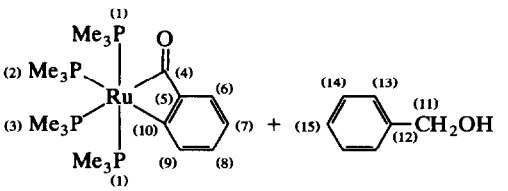

(3)

Complex	^{1}H NMR [b]				^{13}C(^{1}H) NMR [c]			^{31}P{^{1}H} NMR [d]	IR data [e]
	δ	J_{PH}	J_{HH}	Assignment	δ	J_{PC}	Assignment	δ	(cm^{-1})
2	1.10 (vt, 18H)	3.0	–	1	19.6 (vt)	13	1	[A_2MX pattern]	2740(ν_{OH})
	1.42 (d, 9H)	6.8	–	2 or 3	23.0 (d)	18	2 or 3	$-1.4(A_2)(P^1)$	2664(ν_{OH})
	1.43 (d, 9H)	6.0	–	2 or 3	25.3 (d)	26	2 or 3	$6.4(M)(P^2$ or $P^3)$	
	4.66 (s, 2H)	–	–	11	64.3 (s)	–	11	$-14.7(X)(P^2$ or $P^3)$	
	4.83 (brq, 2H)	2.6	–	4	77.6 (d)	11	4	[J_{AM} = 33 Hz]	
	6.72 (m, 3H)	–	[f]	6, 7 and 8	117.3 (s)	–	7 or 8	[J_{AX} = 25 Hz]	
	7.21 (t, 1H)	–	7.0	15	120.2 (s)	–	7 or 8	[J_{MX} = 17 Hz]	
	7.32 (t, 2H)	–	7.0	14	123.0 (s)	–	6		
	7.39 (d, 2H)	–	7.0	13	126.7 (s)	–	15		
	7.47 (m, 2H)	[f]	[f]	9 and OH	127.1 (s)	–	13		
					128.3 (s)	–	14		
					140.7 (s)	–	9		
					144.0 (s)	–	12		
					160.2 (s)	–	5		
					174.7 (dd)	67, 9	10		
3	0.99 (vt, 18H)	3.0	–	1	18.8 (vt, d)	13, 2	1	[A_2MX pattern]	1581 (ν_{CO})
+	1.44 (d, 9H)	7.9	–	2 or 3	22.3 (d)	19	2 or 3	$-3.1(A_2)(P^1)$	
$PhCH_2OH$	1.45 (d, 9H)	6.4	–	3 or 2	25.0 (dt)	27, 2	2 or 3	$9.5(M)(P^2$ or $P^3)$	
	4.34 (t, 1H)	–	5.5	OH	64.7 (s)	–	11	$-14.5(X)(P^2$ or $P^3)$	
	4.66 (d, 2H)	–	5.5	11	121.0 (s)	–	7	[J_{AM} = 35 Hz]	
	6.88 (t, 1H)	–	7.0	8	127.1 (s)	–	13	[J_{AX} = 26 Hz]	
	7.02 (t, 1H)	–	7.0	7	127.2 (s)	–	15	[J_{MX} = 18 Hz]	
	7.22 (t, 1H)	–	7.3	15	128.5 (s)	–	6		
	7.31 (t, 2H)	–	7.3	14	128.5 (s)	–	14		
	7.36 (d, 2H)	–	7.3	13	129.0 (s)	–	8		
	7.47 (d, 1H)	–	7.0	6	141.1 (s)	–	9		
	7.61 (brt, 1H)	[f]	[f]	9	142.8 (s)	–	12		
					143.1 (s)	–	5		
					179.4 (dd)	64, 8	10		
					182.0 (d)	8	4		

[a] All NMR data were collected in CD_2Cl_2 at room temperature. Chemical shifts are reported in ppm and coupling constants in Hz. Multiplicity abbreviations: s, singlet; d, doublet; t, triplet; m, multiplet; vt, virtual triplet; brt, broad triplet; brq, broad quartet; dd, doublet of doublets; dt, doublet of triplets.

[b] At 270.05 MHz. Chemical shifts are referred to Me_4Si as an external standard.

[c] At 67.80 MHz. Chemical shifts are referred to Me_4Si as an external standard.

[d] At 40.26 MHz. Chemical shifts are referred to 85% H_3PO_4 as an external standard.

[e] KBr disc.

[f] Coupling constant was obscure owing to broadening of the signal.

When the catalytic ester formation proceeded, the formation of the ruthenacycloketone **3** was observed. This observation indicates that complex **3** may be derived from an intermediate in the catalytic ester formation. The benzoylruthenium structure of **3** suggests the involvement of its precursor, the benzoyl(benzyloxo)ruthenium **J**. Thus, orthometallation of the benzoyl group in **J** and the subsequent reductive elimination of benzyl alcohol gives **3** [12*]. Complex **J** in the catalytic cycle, on the other hand, forms benzyl benzoate on reductive elimination.

In conclusion, complex **1** having the strongly coordinating PMe_3 ligands showed much weaker catalytic activity than that of $RuH_2(PPh_3)_4$, but the observations obtained with **1** are fairly consistent with the previously proposed mechanism for the $RuH_2(PPh_3)_4$-catalysed dimerization of aldehydes (Scheme 1). However, we cannot exclude at the present stage the possibility of a conventional mechanism for the Tishchenko-type dimerization of aldehydes [2a,j], because in catalytic systems a minor amount of a catalytic species having a high activity is sometimes responsible for the real catalysis rather than an identifiable catalytic species having less activity [13].

4. Experimental details

4.1. General and materials

All manipulations were carried out under an atmosphere of argon or nitrogen or *in vacuo*. ^1H, ^{13}C and ^{31}P NMR spectra were measured on JEOL FX-100 and GX-270 spectrometers. ^1H and ^{13}C signals are referred to Me_4Si as an external standard and ^{31}P NMR signals to 85% H_3PO_4 as an external reference. IR spectra were recorded on a Jasco IR-810 spectrometer. Elemental analysis was carried out by using a Yanagimoto CHN Autocorder type MT-2. Solvents were dried in the usual manners, distilled and stored under an argon atmosphere. Benzaldehyde was obtained from Tokyo Chemical Industry and used without further purification.

$RuH_2(PMe_3)_4$ (**1**) was prepared according to the literature method [6] and identified by NMR and IR spectroscopy and elemental analysis. Anal. Calc. for $C_{12}H_{38}P_4Ru$: C, 35.38; H, 9.40. Found: C, 35.12; H, 9.55%. ^1H NMR (C_6D_6), δ −9.90 (dt, $J = 52$ and 31 Hz, 1H), 1.24 (brd, 18H), 1.34 (brt, 18H); $^{31}P\{^1H\}$ NMR (C_6D_6), δ −1.0 (t, $J = 26$ Hz, 2P), −8.5 (t, $J = 26$ Hz, 2P); IR (KBr disc), 1806 cm^{-1} (ν_{RuH}).

4.2. Preparation of 2

To a toluene solution (2 ml) of $RuH_2(PMe_3)_2$ (**1**) (0.30 g, 0.74 mmol) was added benzaldehyde (0.75 ml, 7.4 mmol) at −78°C. The solution was stirred at −20°C for 16 days and then allowed to stand at the same temperature overnight to give a white precipitate, which was filtered and dried under vacuum. The crude product was dissolved in a minimum amount of toluene at room temperature and cooled to −20°C to form

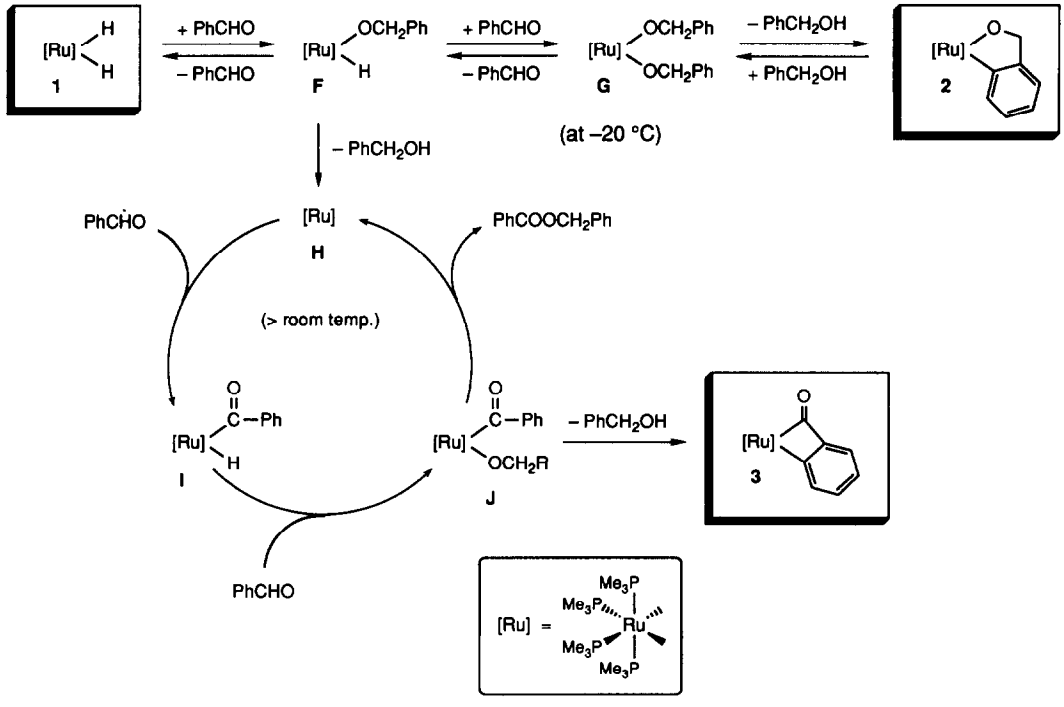

Scheme 2.

colourless crystals of **2** (0.18 g, 40% yield). Anal. Calc. for $C_{19}H_{42}OP_4Ru \cdot C_7H_8O$: C, 50.40; H, 8.13. Found: C, 50.87; H, 7.99%.

4.3. Preparation of 3

To a toluene solution (3 ml) of **1** (0.24 g, 0.59 mmol) was added benzaldehyde (0.6 ml, 5.9 mmol). The solution was stirred at room temperature for 4 days and then at the reflux temperature for 5 h. Cooling the reaction solution to −20°C formed yellow needles of **3**, which were filtered, washed with toluene at −30°C and dried under vacuum (0.12 g, 33% yield). The product contained 1 equivalent of benzyl alcohol in the crystal. Anal. Calc. for $C_{19}H_{40}OP_4Ru \cdot C_7H_8O$: C, 50.56; H, 7.83. Found: C, 50.62; H, 7.81%.

4.4. NMR examination of the reaction of 1 with benzaldehyde

A typical procedure (Table 1, entry 1) is as follows. Complex **1** (138 mg, 0.34 mmol) was placed in an NMR sample tube (10 mm i.d.) equipped with a rubber septum cap and the system was replaced with nitrogen gas. The sample tube was cooled to −70°C and toluene-d_8 (2 ml) and benzaldehyde (0.135 ml, 1.33 mmol) were added. The sample tube was placed in a freezer maintained at −20°C and the reaction system was analysed at intervals by $^{31}P\{^1H\}$ and ^1H NMR spectroscopy. The results are given in Table 1. The ratio of ruthenium complexes in the reaction system was determined based on peak integration in the $^{31}P\{^1H\}$ NMR spectrum. The amounts of organics in the reaction solution were calculated based on the relative intensities of the following peaks with respect to the signals of phenyl protons: PhC*H*O (δ 9.62), $PhCO_2CH_2Ph$ (δ 5.12) and $PhCH_2OH$ (δ 4.73).

4.5. X-ray diffraction study of complex 2

Crystal data: formula $C_{26}H_{50}O_2P_4Ru$, FW = 619.66, orthorhombic, space group $Pnb2_1$, a = 13.580(1) Å, b = 18.220(2) Å, c = 12.540(1) Å, V = 3102.7(5) Å^3, D_c = 1.326 g cm^{-3}, Z = 4, μ (Mo $K\alpha$) = 7.18 cm^{-1}.

A single crystal of dimensions of 0.4 × 0.4 × 0.3 mm was sealed in a glass-made capillary tube and subjected to X-ray diffraction study. Intensity data were collected on a Rigaku AFC5 four-circle diffractometer using graphite-monochromated Mo $K\alpha$ radiation (λ = 0.71068 Å). Unit cell dimensions and an orientation matrix were obtained by a least-squares calculation for 25 automatically centred reflections in the range $20 \leq 2\theta \leq 25°$. Diffraction intensities were measured at 19°C in the range $3 \leq 2\theta \leq 60°$ ($+h$, $+k$, $+l$) using the ω–2θ scan technique at a scan rate of 4° min^{-1} in ω. Three standard reflections, measured at every 100 reflection measurements, showed no appreciable decrease in the intensities during the data collection. No absorption correction was made. Of the 4675 unique reflections measured, 2715 were classed as observed ($F_o > 3\sigma(F_o)$) and these were used for the solution and refinement of the structure.

Calculations were performed on a FACOM A70 computer using the R-CRYSTAN program. The structure was solved by a combination of direct methods (SAPI85) and Fourier techniques. Hydrogen atoms were not located. The structure was refined by full-matrix least-squares calculations with anisotropic thermal parameters for the oxaruthenacycle moiety and with isotropic thermal parameters for the benzyl alcohol moiety. The final R value was 0.070 (R_w = 0.066). The bond distances and angles are listed in Table 2. Atomic coordinates and equivalent isotropic and isotropic thermal parameters are given in Table 4.

TABLE 4. Atomic coordinates with equivalent isotropic temperature factors for the oxaruthenacycle complex **2**

Atom	x	y	z	B_{eq} [a]
Ru	0.04520(0)	0.42567(3)	0.26714(6)	2.15(1)
P1	0.0489(10)	0.5315(2)	0.3783(3)	3.91(9)
P2	0.0432(9)	0.4909(2)	0.1121(3)	3.18(8)
P3	−0.1243(7)	0.4093(6)	0.2669(7)	3.4(2)
P4	0.2204(6)	0.4096(5)	0.2532(7)	3.3(2)
O1	0.038(2)	0.3678(5)	0.4159(7)	3.9(3)
C1	0.048(3)	0.2899(7)	0.413(1)	4.6(4)
C2	0.058(1)	0.2648(6)	0.299(1)	2.2(3)
C3	0.051(3)	0.1876(6)	0.281(1)	3.6(3)
C4	0.035(2)	0.1597(7)	0.178(1)	3.7(5)
C5	0.048(2)	0.2090(7)	0.091(1)	4.5(4)
C6	0.037(2)	0.2864(7)	0.110(1)	3.2(4)
C7	0.045(2)	0.3151(6)	0.2153(9)	3.0(3)
C8	0.162(2)	0.565(1)	0.441(2)	9.2(10)
C9	−0.029(2)	0.512(1)	0.500(2)	7.3(7)
C10	−0.005(2)	0.6216(9)	0.342(2)	7.6(8)
C11	−0.060(2)	0.549(1)	0.089(2)	3.9(7)
C12	0.147(2)	0.560(1)	0.085(3)	5.3(8)
C13	0.044(3)	0.4451(8)	−0.020(1)	5.5(5)
C14	−0.216(3)	0.493(2)	0.286(3)	6.1(9)
C15	−0.170(2)	0.342(2)	0.351(2)	5.0(9)
C16	−0.178(2)	0.373(2)	0.149(2)	3.6(6)
C17	0.271(2)	0.344(1)	0.370(2)	7.6(6)
C18	0.262(2)	0.369(2)	0.120(2)	5.6(7)
C19	0.313(2)	0.476(2)	0.284(3)	4.7(7)
O2	0.174(1)	0.3948(7)	0.573(1)	6.7*
C20	0.135(2)	0.360(1)	0.663(2)	5.8*
C21	0.209(2)	0.306(1)	0.713(2)	4.8*
C22	0.201(2)	0.289(1)	0.819(2)	6.2*
C23	0.270(2)	0.237(2)	0.864(2)	7.7*
C24	0.341(2)	0.207(1)	0.807(2)	5.9*
C25	0.353(2)	0.227(2)	0.699(2)	7.0*
C26	0.286(2)	0.275(1)	0.649(2)	5.9*

[a] $B_{eq} = (8\pi^2/3)\Sigma_i\Sigma_j[U_{ij}a_i^*a_j^*(\mathbf{a}_i \cdot \mathbf{a}_j)]$. Asterisks denote B values that are isotropic.

Acknowledgements

The authors are grateful for the support of this work by the Ministry of Education, Science and Culture and by Nippon Zeon Co.

References and notes

1 T. Ito, H. Horino, Y. Koshiro and A. Yamamoto, *Bull. Chem. Soc. Jpn., 55* (1982) 504; H. Horino, T. Ito and A. Yamamoto, *Chem. Lett.*, (1978) 17.

2 For other examples of transition metal-catalysed Tishchenko-type reactions, see: (a) M. Yamashita, Y. Watanabe, T. Mitsudo and Y. Takegami, *Bull. Chem. Soc. Jpn., 49* (1976) 3597; (b) S. Komiya, S. Taneichi, A. Yamamoto and T. Yamamoto, *Bull. Chem. Soc. Jpn., 53* (1980) 673; (c) S. Murahashi, K. Ito, T. Naota and Y. Maeda, *Tetrahedron Lett., 22* (1981) 5327; (d) G.M. Villacorta and J.S. Filippo, Jr., *J. Org. Chem., 48* (1983) 1151; (e) K.A. Bernard and J.D. Atwood, *Organometallics, 7* (1988) 235 and *8* (1989) 795; (f) K. Yokoo, N. Mine, H. Taniguchi and Y. Fujiwara, *J. Organomet. Chem., 279* (1985) C19; (g) E.R. Burkhardt, R.G. Bergman and C.H. Heathcock, *Organometallics, 9* (1990) 30; (h) N. Menashe and Y. Shvo, *Organometallics, 10* (1991) 3885; (i) V.V. Grushin and H. Alper, *J. Org. Chem., 56* (1991) 5159; (j) K. Morita, Y. Nishiyama and Y. Ishii, *Organometallics, 12* (1993) 3748.

3 S.D. Ittel, C.A. Tolman, A.D. English and J.P. Jesson, *Adv. Chem. Ser., 173* (1979) 67; J.W. Suggs, *J. Am. Chem. Soc., 100* (1978) 640; D. Milstein, *Organometallics, 1* (1982) 1549; J.A. Gladysz, *Adv. Organomet. Chem., 20* (1982) 1; D.L. Thorn, *J. Mol. Catal., 17* (1982) 279; K.L. Brown, G.R. Clark, C.E.L. Headford, K. Marsden and W. Roper, *J. Am. Chem. Soc., 101* (1979) 503; D.R. Fahey, *J. Am. Chem. Soc., 103* (1981) 136; T.B. Rauchfuss, *J. Am. Chem. Soc., 101* (1979) 1045; D. Milstein, *J. Chem. Soc., Chem. Commun.*, (1982) 1357; C.G. Anklin, P.S. Pregosin, F.J. Wombacher and H.J. Rüegg, *Organometallics, 9* (1990) 1953; A.J. Arce, Y. De Sanetis and A. Deeming, *J. Organomet. Chem., 311* (1986) 371; C. Bianchini, A. Meli, M. Peruzzini, A. Vacca and F. Zanobini, *Organometallics, 6* (1987) 2453; C. Bianchini, A. Meli, M. Peruzzini and F. Vizza, *Organometallics, 10* (1991) 820; C. Bianchini, A. Meli, M. Peruzzi, J.A. Ramirez, A. Vacca, F. Vizza and F. Zanobini, *Organometallics, 8* (1989) 337; K.I. Hardcastle, H. Minassian, A.J. Arce, Y. De Sanetis and A.J. Deeming, *J. Organomet. Chem., 368* (1989) 119.

4 (a) Y. Hayashi, S. Komiya, T. Yamamoto and A. Yamamoto, *Chem. Lett.*, (1984) 1363; (b) P.W.N.M. van Leeuwen and C.F. Roobeek, *Organometallics, 9* (1990) 2179; (c) K. Tani, E. Tanigawa, Y. Tatsuno and S. Otsuka, *J. Organomet. Chem., 279* (1985) 87; (d) H.E. Bryndza and W. Tam, *Chem. Rev., 88* (1988) 1163, and references cited therein.

5 S. Komiya, Y. Akai, K. Tanaka, T. Yamamoto and A. Yamamoto, *Organometallics, 4* (1985) 1130; A. Yamamoto, T. Yamamoto and F. Ozawa, *Pure Appl. Chem., 57* (1985) 1799, A. Yamamoto, *Adv. Organomet. Chem., 34* (1992) 111, and references cited therein.

6 R.A. Jones, G. Wilkinson, I.J. Colquohoun, W. McFarlane, A.M.R. Galas and M.B. Hursthouse, *J. Chem. Soc., Dalton Trans.*, (1980) 2480.

7 P. Schuster, G. Zundel and C. Sandorfy (eds.), *The Hydrogen Bond. II. Structure and Spectroscopy,* North-Holland, Amsterdam, 1976.

8 For leading references of transition metal alkoxides associated with alcohol by a hydrogen bond, see: (a) Y.-J. Kim, K. Osakada, A. Takenaka and A. Yamamoto, *J. Am. Chem. Soc., 112* (1990) 1096; (b) K. Osakada, K. Ohshiro and A. Yamamoto, *Organometallics, 10* (1991) 404.

9 For examples of ruthenium alkoxides, see: refs. 4a and 8b; T.J. Johnson, J.C. Huffman and K.G. Caulton, *J. Am. Chem. Soc., 114* (1992) 2725; S.D. Loren, B.K. Campino, R.H. Heyn, T.D. Tilley, B.E. Bursten and K.W. Kuth, *J. Am. Chem. Soc., 111* (1989) 4712, and references cited therein.

10 The assignments in the ^{1}H and ^{13}C NMR were performed by H–H and H–C COSY techniques. The $^{31}P\{^{1}H\}$ NMR data were confirmed by spin-simulation experiments (LAOCN98).[11]

11 K. Satake, *Kagaku (Chemistry)*, Kagakudojin, Kyoto, 1984; Vol. 39, Nos. 9 and 10, Appendix.

12 According to the reaction processes in Scheme 2, the formation of **3** from **1** and benzaldehyde is accompanied by the formation of 2 equivalents of benzyl alcohol. The amount of benzyl alcohol formed in entry 3 in Table 1 (256%/**3**) is in agreement with the stoichiometry.

13 J. Halpern, *Science (Washington, DC), 217* (1982) 401.